How unnatural amino acids in antimicrobial peptides change interactions with lipid model membranes

Saheli Mitra[1], Mei-Tung Chen[1], Francisca Stedman[1], Jedidiah Hernandez[1], Grace Kumble[1], Xi Kang[1], Churan Zhang[1], Grace Tang[1], Ian Daugherty[1], Alice Liu[1], Jeremy Ocloo[1], Kevin Raphael Klucznik[1], Alexander Anzhi Li[1], Frank Heinrich[1,2], Berthony Deslouches[3], Stephanie Tristram-Nagle[1]

[1]Biological Physics Group, Physics Department, Carnegie Mellon University, Pittsburgh, PA 15213, USA; [2]Center for Neutron Research, National Institute of Standards and Technology, Gaithersburg, MD 20899, USA; [3]Department of Environmental and Occupational Health, University of Pittsburgh, Pittsburgh, PA 15261, USA

*Corresponding author's email: stn@cmu.edu

ABSTRACT

This study investigates the potential of antimicrobial peptides (AMPs) as alternatives to combat antibiotic resistance, with a focus on two AMPs containing unnatural amino acids (UAAs), E2-53R (16 AAs) and LE-54R (14 AAs). In both peptides, valine is replaced by norvaline (Nva), and tryptophan is replaced by 1,2,3,4-Tetrahydroisoquinoline-3-carboxylic acid (Tic). Microbiological studies reveal their potent activity against both Gram-negative (G(-)) and Gram-positive (G(+)) bacteria without any toxicity to eukaryotic cells. Circular dichroism (CD) spectroscopy indicates that these peptides maintain α-helical structures when interacting with G(-) and G(+) lipid model membranes (LMMs), a feature linked to their efficacy. X-ray diffuse scattering (XDS) demonstrates a softening of G(-), G(+) and eukaryotic (Euk33) LMMs and a decrease in chain order as a potential determinant for bacterial destabilization. Additionally, XDS finds a significant

link between both peptides' interfacial location in G(-) and G(+) LMMs and their efficacy. Neutron reflectometry (NR) confirms the AMP locations determined using XDS. Both AMPs with UAAs offer a promising strategy to combat antibiotic-resistant strains while preserving human cell integrity. These findings are compared with previously published data on E2-35, which consists of the natural amino acids arginine, tryptophan, and valine.

KEYWORDS

Gram-negative(G(-)), Gram-positive (G(+)), lipid model membranes (LMMs), circular dichroism (CD), X-ray diffuse scattering (XDS), neutron reflectometry (NR)

INTRODUCTION

Peptides are attractive candidates for therapeutic applications due to their ability to achieve a high degree of chemical diversity. Peptide-containing drugs have been successfully developed and are widely used in clinical practice.[1-2] Natural peptides are multifunctional mediators of the innate immune response, with some direct antimicrobial activity and diverse immunomodulatory properties.[3-5] Inspired by naturally occurring antimicrobial peptides (AMPs), scientists have created synthetic versions of AMPs as potential substitutes for conventional antibiotics.[6-8] Both natural and synthetic AMPs have shown strong and broad-spectrum antibacterial properties in laboratory studies and have been effective in various animal infection models. [9-10] Importantly, their effectiveness is believed to be unaffected by the typical mechanisms of bacterial resistance that render many traditional antibiotics ineffective.[11-17] Therefore, AMPs represent a potential solution to the challenge of treating infections caused by multi-drug resistant (MDR) bacteria.

In general, AMPs are small in size (12–50 amino acid residues) with an overall cationic (a net positive charge of +2 to +13) and amphipathic structure. [5, 18-19] Several models have been suggested to explain how AMPs work against bacteria, with most emphasizing the disruption of cell membranes. Cationic AMPs are drawn to the negatively charged surface of bacterial cells, which is the basis for their bacterial selectivity.[20] Despite thorough research, the exact ways in which AMPs interact with membranes and kill bacteria remain unclear for many of these peptides. One hypothesis is that when AMPs are added to a suspension of bacterial cells, they undergo "self-promoted uptake" into the cells, crossing the outer membrane or cell wall. [21] This is followed by disrupting the inner membrane, which ultimately leads to bacterial cell death. [22-26] AMPs may create pores in the membrane [27-29], which can take shapes like "barrel-stave" or "toroidal". [30-32] Alternatively, AMPs can exhibit actions such as interfacial activity [33], thinning the membrane [34-36], segregating lipid domains [37], or solvation (referred to as the "carpet" model). [38-39] While membrane disruption is often seen as the primary mechanism of action for AMPs, other processes like inhibition of cell wall biosynthesis,[40-41] cell division, and lipopolysaccharide transport [42-43] may also contribute to their antibacterial effectiveness. These topics have been discussed in recent reviews by Hancock et al. [44-46]

Recent scientific progress has highlighted the potential to enhance the effectiveness and specificity of cationic AMPs. One strategy involves strategically selecting specific combinations of amino acids. For instance, incorporating positively charged arginine (Arg, R) residues on one face of the helix and hydrophobic valine (Val, V) residues on the other face can improve selectivity. Additionally, extending the peptide chain length and introducing tryptophan (Trp, W) on the hydrophobic face of a helical peptide can enhance antimicrobial activity. [19, 47-49] However, a key challenge in AMP design is balancing antibacterial efficacy with host toxicity. To address this, a

systematic approach adjusts the length and sequence of specific amino acids. [50] Some studies caution against using W exclusively in the hydrophobic domain due to its high hydrophobicity and bulky indole ring, which can increase host toxicity. [48, 51] To mitigate this, we added three, four or five Ws to the remaining Vs in the hydrophobic domain in our previous studies. [50, 52-53] Despite these advancements, the transition of AMPs from the lab to the market faces obstacles like rapid degradation by plasma and bacterial proteases, as well as fast hepatic and renal clearance, resulting in short half-lives and loss of antimicrobial activity. [54] Researchers have explored various strategies to enhance AMP stability, including incorporating unnatural amino acids (UAAs), N- and/or C-terminal modifications, cyclization, and multimerizing AMP monomers. [55-62] UAAs include those amino acids that are excluded from the canonical genetic code, originating either from natural or synthetic sources.[63] Numerous studies have reported that the introduction of UAAs significantly enhanced their antimicrobial efficacy and proteolytic stability.[63-71]

In the present study we aimed to design peptides with enhanced antibacterial activity and proteolytic resistance with low cytotoxicity. For that we developed two peptides LE-54R (14-mer), and E2-53R (16-mer) which is the derivative of E2-35 [53], in which Ws and Vs are replaced by 1,2,3,4-tetrahydroisoquinoline-3-carboxylic acid (Tic) and Norvaline (Nva). The chemical structures of the unnatural amino acids are shown in Figure 1. The amino acid sequences and physical attributes of E2-53R and LE-54R are provided in Table 1, where R denotes a peptide containing a UAA. The secondary structures of the AMPs were analyzed using circular dichroism (CD) measurements to explore potential correlations with their activity. To investigate the effect of these AMPs on the structure of membranes, XDS was employed to determine their location within different LMMs, as well as their effect on membrane rigidity and lipid chain order. Neutron reflectometry (NR) experiments served to validate the X-ray findings. Through *in vitro*

microbiological assays, the antibacterial activity and cytotoxicity of E2-53R and LE-54R were determined.

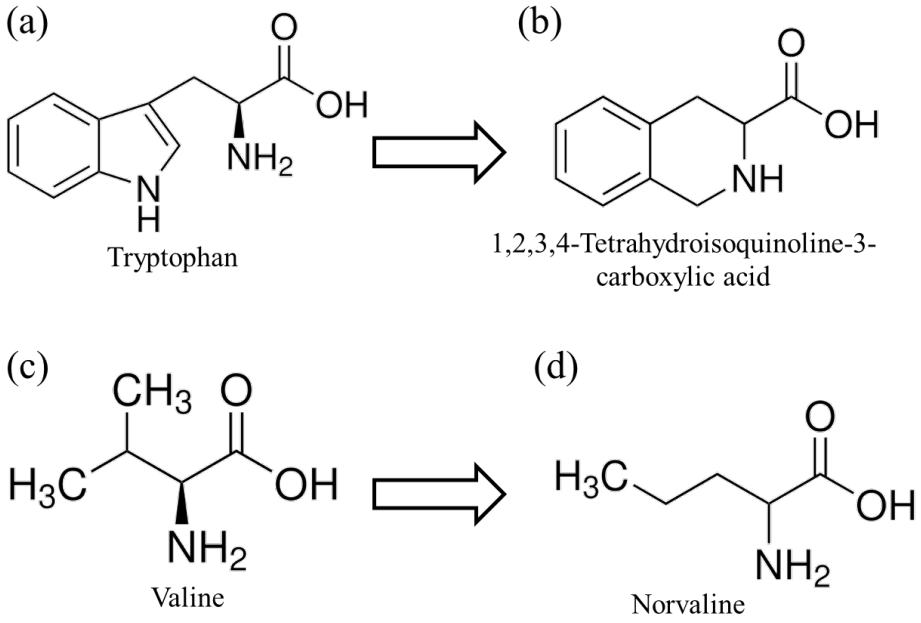

Figure 1. Chemical structures of amino acids. (a) Tryptophan is replaced by (b) 1,2,3,4-Tetrahydroisoquinoline-3-carboxylic acid (Tic (X)) and (c) Valine is replaced by (d) Norvaline (Nva (U)).

Table 1. Amino acid sequences of E2-35[53], E2-53R and LE-54R and their physical attributes. The charged residues are bolded. The hydrophobicity (H) and hydrophobic moment (μH) were determined using the online software HeliQuest (http://heliquest.ipmc.cnrs.fr).

Peptide	Amino acid sequence	# residues	Charge	μH	H	μH/H
E2-35	**RR** VW **RW** V**R** **RV** W**R** WV **RR**	16	+8	0.736	0.363	2.03
E2-53R	**RR** UX **RX** U**R** **RU** X**R** XU **RR**	16	+8	0.713	0.338	2.11
LE-54R	**RR** **RR** **RR** **RX** XX XU UU	14	+7	0.037	0.378	0.09

EXPERIMENTAL

Materials

The synthetic lyophilized lipids 1-palmitoyl-2-oleoyl-*sn*-glycero-3-phosphoethanolamine (POPE), 1-palmitoyl-2-oleoyl-*sn*-glycero-3-phospho-(10-rac-glycerol) sodium salt (POPG), 10,30-bis[1,2-dioleoyl-*sn*-glycero-3-phospho]-*sn*-glycerol sodium salt (TOCL, i.e., cardiolipin), 1-stearoyl-2-oleoyl-sn-glycero-3-phosphocholine (SOPC), 1-palmitoyl-2-linoleoyl-sn-glycero-3-phosphocholine (PLPC), egg sphingomyelin (ESM), and 1,2-dioleoyl-3-trimeathylammoniumpropane chloride salt (DOTAP) were purchased from Avanti Polar Lipids (Alabaster, AL) and used as received. Cholesterol was from Nu-Chek-Prep (Waterville, MN). HPLC-grade organic solvents were purchased from Sigma-Aldrich (St. Louis, MO). Lipid stock solutions in chloroform were combined to create lipid mixtures in molar ratios mimicking the G(-) inner membrane (IM): POPE/POPG/TOCL (7:2:1 molar ratio), G(+) membrane: POPG/DOTAP/POPE/TOCL (6:1.5:1.5:1),[72] and eukaryotic membrane, Euk33: SOPC/PLPC/POPE/ESM/cholesterol (15:10:5:3:16.5) (33 mole % cholesterol).[73] Bacterial cation-adjusted Mueller Hinton Broth (MHB2), Test Condition Media, Roswell Park Memorial Institute (RPMI) media, fetal bovine serum (FBS) and phosphate-buffered saline (PBS) were obtained from Millipore Sigma (St Louis, MO). RPMI media contains the reducing agent glutathione as well as biotin, vitamin B12, and para aminobenzoic acid. In addition, RPMI media includes high concentrations of the vitamins inositol and choline. Because RPMI contains no proteins, lipids, or growth factors, it is commonly supplemented with FBS. FBS contains more than 1,000 components such as growth factors, hormones, and transport proteins that contribute to cell growth when supplemented into culture media.[74] Formaldehyde was obtained from ThermoFisher (Waltham, MA). The peptides E2-53R (MW: 2979 gm/mol) and LE-54R (MW: 2836 gm/mol)

were purchased in lyophilized form (10 mg in a 1.5 mL vial) from Genscript (Piscataway, NJ) with HPLC/MS spectra corresponding to each designed primary sequence. The traditional antibiotics and colistin were purchased from Millipore Sigma (St. Louis, MO). Amino acid sequences of the peptides and their physical attributes are provided in Table 1.

METHODS

Antibacterial assay

Bacterial clinical isolates used for initial screening were anonymously provided by the clinical microbiology laboratory of the University of Pittsburgh Medical Center (UPMC). Bacteria were stored at –80 °C and typically retrieved by obtaining single colonies on agar plates prior to subsequent liquid broth culture. Suspensions of test bacteria were prepared from the log phase of growth by diluting overnight cultures at 1:100 with fresh cation-adjusted MHB2 and incubating for an additional 3–4 h. Bacteria were spun at 3,000 *g* for 10 min. The pellet was resuspended in Test Condition Media to determine bacterial turbidity using a Den-1B densitometer (Grant Instruments, Beaver Falls, PA) at 0.5 McFarland units corresponding to 10^8 CFU/mL.

To examine antibacterial activity, we used minor modifications of a standard growth inhibition assay endorsed by the Clinical and Laboratory Standards Institute (CLSI), as previously described.[75] Bacteria were incubated with each of the indicated peptides in MHB2. The bacterial cells were kept in an incubator for 18 h at 37 °C, which is linked to a robotic system that feeds a plate reader every hour with one of 8 × 96-well plates. The 96-well plates are standard flat-bottom microliter plates purchased from Thermo Fisher (Waltham, MA). This setup allows the collection of growth kinetic data at A 570 (absorbance at 570 nm) to examine growth inhibition in real-time (BioTek Instruments, Winooski, VT). We define minimum inhibitory concentration (MIC) as the

minimum peptide concentration that completely prevents bacterial growth, demonstrated by a flat (horizontal line) growth curve as a function of hourly determinations for 18 hrs. at A570.[50, 75] The assays are typically repeated a second time. If the MIC differs from the first assay, a third experimental trial is performed to confirm the MIC.

Determination of toxicity to mammalian cells

Toxicity to eukaryotic cells was examined using human red blood cells (RBCs) and peripheral mononuclear cells (PBMC or white blood cells (WBCs)) as previously described.[50, 76] Briefly, RBCs and WBCs were separated by histopaque differential centrifugation using blood anonymously obtained from the Central Blood Bank (Pittsburgh, PA). For the RBC lysis assay, the isolated RBCs were resuspended in PBS at a concentration of 5%. The peptides were serially diluted twofold in 100 μL of PBS before adding 100 μL of 5% RBC to a final dilution of 2.5% RBC to ensure that the A570 of hemoglobin did not saturate the plate reader. In parallel, the RBCs were osmotically burst with water at increasing concentrations to generate a standard curve of RBC lysis. Three technicians independently conducted experiments to ensure reproducibility.

Human WBCs RPMI and 10% FBS were incubated with each selected peptide for 1 h at 37 °C. The cells were then immediately washed with PBS at 1,000 *g* for 7 min, while in a round-bottom 96-well plate. After resuspension in PBS, fixable blue live/dead stain from Life Technologies was added according to manufacturer's instructions. The cells were again washed and resuspended in PBS to remove non-specific stain and then fixed with 4 % formaldehyde for 1 h. After washing again with PBS, the samples were stored at 4 °C overnight (in the dark) before examination by flow cytometry using the Novocyte flow cytometer (Agilent Technologies, Santa Clara, CA). Peptide-treated cells were compared with untreated cells for dye incorporation, and

data were analyzed using the Novocyte analytical software. Dye incorporation was quantified as percent toxicity directly determined by distinguishing live from dead populations,[76] which was plotted using GraphPad (Prizm software, San Diego, CA).

Circular dichroism (CD)

Unilamellar vesicles (ULVs) of ~ 600 Å diameter were prepared using an extruder (Avanti Polar Lipids, Alabaster, AL). 250 µL of 20 mg/mL multilamellar lipid vesicles was extruded 21 times through a single Nucleopore filter of size 500 Å using 0.2 mL Hamilton syringes. The final lipid concentration in the ULVs was 18 mg/mL as determined gravimetrically. Concentrated ULVs were added to 3 mL of 10 µmol/L (µM) peptide in 15 mM PBS at pH 7 to create lipid/peptide molar ratios between 0:1 and 70:1. Higher molar ratios of lipid:peptide were not possible due to absorption flattening in the UV region. The samples remained at room temperature for ~1-4 hours before the CD measurement. Data were collected in 3 mL quartz cuvettes using a Jasco 1500 CD spectrometer at 37 ºC in the Chemistry Department at Carnegie Mellon University. The samples were scanned from 200 to 240 nm 20 times and the results averaged. The temperature was controlled at 37 °C via a Peltier element with water circulation through the sample compartment. Nitrogen gas was used at a flow rate between 0.56 and 0.71 m^3/h to protect the UV bulb. OriginPro 2024 (OriginLab, Northampton, MA) was used to carry out a Levenberg–Marquardt least squares fit of the tryptophan-subtracted ellipticity traces to four secondary structural motifs representing α-helix, β-sheet, β-turn and random coil.[34, 77] This analysis gives a percentage match of each secondary structural motif to the total sample ellipticity. Instrument ellipticity (ε) was converted to Mean Residue Ellipticity using MRE (deg $cm^2/dmol$) = $\varepsilon \times 10^4/N$, where N = # amino acids and peptide concentration was always 10 µM.

Low-angle x-ray diffuse scattering (XDS)

Oriented samples consisting of stacks of approximately ~1800 bilayers were prepared using the well-established "rock and roll" method.[78] 4 mg of lipids and peptides in organic solvent, chloroform:methanol (2:1, v/v) or trifluoroethanol:chloroform (1:1, v/v), were deposited onto a Si wafer (15mm W × 30 mm L × 1 mm H) inside a fume hood. After rapid evaporation while rocking the substrate, an immobile film formed which was then further dried inside the fume hood for two hours, followed by overnight drying under vacuum to evaporate residual organic solvent. The samples were trimmed to occupy 5 mm W × 30 mm L along the center of the Si substrate. The substrate was fixed to a glass block (10 mm H × 15 mm W × 32 mm L) using heat sink compound (Dow Corning, Freeland, MI). The sample was stored in a refrigerator at 4 ^{o}C for several hours. Cold storage prior to transfer into a well-insulated hydration chamber held at 37 ^{o}C caused 100% hydration through the vapor within just 10 minutes. This process is faster than our previous method that required a Peltier cooler under the sample.[79] Low-angle XDS (LAXS) data from oriented, fully hydrated samples were obtained at the ID7B2 line at Center for High Energy X-ray Sciences (CHEXS, Ithaca, NY) on two separate trips to the Cornell High Energy Synchrotron Source (CHESS) using X-ray wavelengths of 0.8855 Å and 0.8856 Å, sample-to-detector (S)-distances of 401 mm and 400.1 mm, beam size 0.25mm H and 0.35 mm V, with an Eiger 16M detector. 30-second exposures were carried out in the fluid phase at 37 °C. The flat silicon wafer was rotated from -1 to 6 degrees during the data collection at CHESS to equally sample all angles of incidence. The background was collected by setting the x-ray angle of incidence to -2.0 degrees, where sample scattering does not contribute to the image. For data analysis, backgrounds were first subtracted to remove extraneous air and mylar scattering and the images were laterally symmetrized to increase the signal-to-noise ratio. As the sample nears full hydration, membrane

fluctuations occur which produce ‘‘lobes’’ of diffuse x-ray scattering data.[80] The fluctuations are quantitated by measuring the fall-off in lobe intensity in the lateral q_r direction. The fitting procedure is a non-linear least squares fit that uses the free energy functional from liquid crystal theory,[81]

$$f = \frac{\pi}{NL_r^2} \int r\, dr \sum_{n=0}^{N-1} \{K_C[\Delta_r^2 u_n(r)]^2 + B[u_{n+1}(r) - u_n(r)]^2\} \qquad (1)$$

where N is the number of bilayers in the vertical (Z) direction, L_r is the domain size in the horizontal (r) direction, and K_C is the bending modulus. K_C describes the bending of an average, single bilayer where u_n is the vertical membrane displacement and B is the compressibility modulus. A higher K_C indicates a stiffer membrane, and a lower K_C indicates a softer membrane.

Wide-angle XDS

Wide-angle XDS (WAXS) was obtained at CHESS. In order to obtain WAXS data, the same sample that was hydrated for LAXS is x-rayed with a fixed glancing angle of incidence, instead of a rotation of the sample. In order to remove significant water scattering in the wide-angle region, a gentle nitrogen stream was introduced into the hydration chamber during continuous WAXS data collection. Two exposures are taken at angles of x-ray incidence $\alpha = +0.3^0$ and $\alpha = -0.3^0$, where the negative angle image is then subtracted from the positive angle image. Both are 30-second scans. The subtraction procedure removes extraneous scatter due to the mylar chamber windows and shadows. The chain–chain correlation appears as strong diffuse scatter projecting upwards circularly from the equator; the fall-off in intensity yields information about chain order. To obtain an S_{xray} order parameter the intensity is first integrated along its radial trajectory, then fit to wide-angle liquid crystal theory.[82] The chain scattering model assumes long thin rods that are locally well aligned along the local director (n_L), with orientation described by the angle β. While acyl

chains from lipids in the fluid phase are not long cylinders, the model allows the cylinders to tilt (β) in a Mauer-Saupe distribution to approximate chain disorder. From the fit of the intensity data using a Matlab computer program,[83] we obtain S_{xray} using Eqn. (2):

$$S_{xray} = \frac{1}{2}(3\langle cos^2\beta\rangle - 1) \qquad (2)$$

We also obtain the RMSE (root mean square error), which reports the goodness of the fit.

Neutron Reflectivity (NR)

NR measurements were performed at the OFFSPEC reflectometer at the ISIS Neutron and Muon Source, Rutherford Appleton Laboratory, Didcot, United Kingdom.[84] Reflectivity curves were recorded at 37 ºC temperature for momentum transfer values 0.01 $Å^{-1} \leq q_z \leq 0.33$ $Å^{-1}$. The neutron sample cells allow *in situ* buffer exchange, and a series of measurements on the same bilayer under different isotopic solutions (pure H_2O and D_2O) were performed on the same sample. 6 mg lipid/peptide mixtures were co-solubilized in chloroform, dried under vacuum and then hydrated for 1-2 hours via bath sonication in 1.2 mL 2M NaCl, thereby creating peptide-containing lipid vesicles. Sparsely-tethered lipid bilayer membranes (stBLMs) were prepared on smooth gold-coated (~140 Å film thickness, 4 Å - 9 Å r.m.s surface roughness) silicon wafers by immersing them in a 70:30 mol:mol β-mercaptoethanol:HC18 tether solution in ethanol for at least 60 min, leading to the formation of a self-assembled monolayer (SAM) of both molecules at the gold surface.[85] SAM-decorated wafers were assembled in the NR cell, and lipid bilayers were completed by fusing vesicles of the desired lipid/peptide mixtures using an osmotic shock procedure.[86] NR data were sequentially collected after rinsing the NR cell with ~6 cell volumes of either D_2O or H_2O-based using a syringe. NR datasets collected on stBLMs immersed in isotopically different solutions were analyzed simultaneously (2 datasets per stBLM). One-

dimensional structural profiles of the substrate and the lipid bilayer along the interface normal *z* were parameterized with a model that utilizes continuous volume occupancy distributions of the molecular components.[87] Free-form peptide profiles were modeled using Hermite splines with control points on average 15 Å apart.[88] The protein extension along the membrane normal determines the number of spline control points and was iteratively refined. A Monte Carlo Markov Chain-based global optimizer was used to determine best-fit parameters and their confidence limits.

RESULTS AND DISCUSSION

Antibacterial activity

E2-53R and LE-54R were initially screened for antibacterial potency against an MDR panel of G(-) and G(+) bacterial isolates from University of Pittsburgh medical Center (UPMC). The MIC is measured by a horizontal growth curve taken every hour [50]; these MIC values are plotted in Figure 2 (a) and (b). Additionally, MIC values for the previously reported E2-35 peptide are included for comparison.[53] The MICs represent the average of different strains of each species of bacteria. Remarkably, both R peptides exhibited broad-spectrum activity against both G(-) and G(+) bacterial species, surpassing tobramycin (a conventional antibiotic) with the lowest MIC values. Both peptides demonstrated similar efficacy against G(-) and G(+) bacteria, however overall MICs are lower in G(+) bacteria compared to G(-) bacteria. E2-53R demonstrated inferior antibacterial activity compared to its counterpart E2-35[53] in G(-) bacteria, however, in G(+) the bactericidal activity of both these peptides were similar.

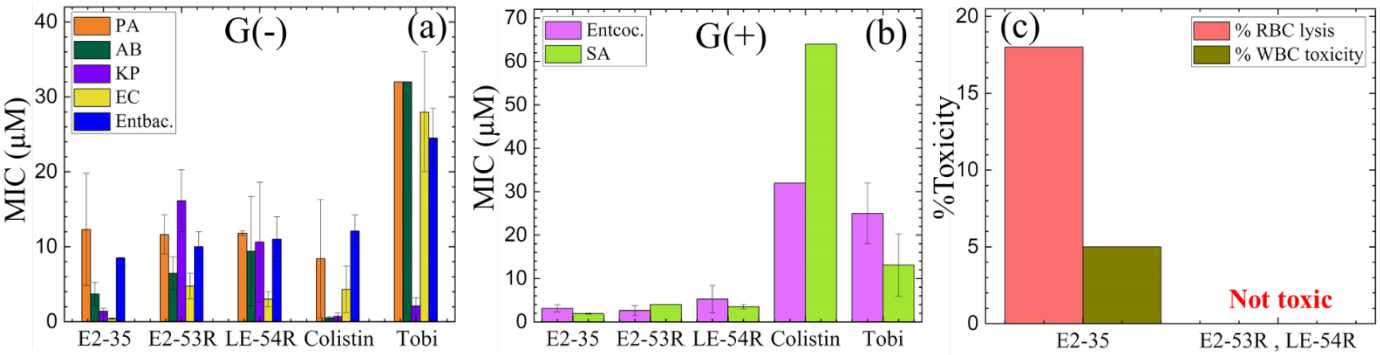

Figure 2. Antibacterial activity and toxicity of E2-35 , E2-53R and LE-54R peptides and controls. Selected peptides were examined for MIC against **(a)** G(–) and **(b)** G(+) MDR isolates from UPMC. Abbreviations: G(–): *Pseudomonas aeruginosa* (PA), *Acinetobacter baumannii* (AB), *Klebsiella pneumoniae* (KP), *Escherichia coli* (EC), *Enterobacter* (Entbac). G(+): *Enterococci faecalis* (Entcoc.) and *Staphylococcus aureus* (SA). The MICs are the average strains of each type of bacteria. **(c)** % Red blood cell (RBC) lysis at 32 μM and % toxicity at 16 μM against freshly isolated human white blood cells (WBCs) were determined by live–dead stain incorporation using flow cytometry. Maximum test concentrations (MTCs) are limited to 16 or 32 μM to ensure each peptide is available for iterative structure–function testing against large panels of antibiotic-resistant clinical isolates. Data are representative of 2–3 experimental trials. Error bars correspond to standard error of the mean values, σ = Std. dev/$\sqrt{N}$. Std. devs are calculated by combining the standard deviations for each bacterial species, $\sigma_{Ave} = \sqrt{((\sigma_A)^2 + (\sigma_B)^2 + (\sigma_C)^2\ldots)}/N$. E2-35 data were adapted from our previously published paper [53] with permission.

To compare Minimum Inhibitory Concentration (MIC) values with physical characteristics, we utilized the HeliQuest website (https://heliquest.ipmc.cnrs.fr) [89-91] to compute hydrophobicity (H) and hydrophobic moment (μH). The physical attributes of both the peptides are listed in Table 1. Despite LE-54R having one less R and V compared to E2-53R, it didn't notably alter the H values, but the μH value was markedly higher in E2-53R than in LE-54R. Given that both peptides exhibit similar bactericidal activity, it seems that the influence of physical attributes on MIC is negligible in this context. While these calculations are informative, we propose that changes in physical attributes are less crucial than secondary structural alterations of the AMPs and structural modifications in the LMMs.

Toxicity to eukaryotic cells

We conducted a thorough assessment of the lytic activity of all peptides to evaluate their potential harm to eukaryotic cells, particularly red blood cells (RBCs) and white blood cells (WBCs). The data we obtained, as illustrated in Figure 2 (c), indicates that neither of the peptides causes any noticeable toxicity to eukaryotic cells. The presence of cholesterol in the eukaryotic membrane in general reduces the activity of antimicrobial peptides, due to either stabilization of the lipid bilayer or to interactions between cholesterol and the peptide. [92-93] This underscores their promising prospects for therapeutic use. This finding contrasts to our previously reported peptide, E2-35, which exhibited some degree of toxicity.[53] This is a significant observation as it demonstrates that replacing W and V with UAAs Tic and Nva eliminates toxicity to eukaryotic cells.

Secondary structure

A plot of the % α-Helix vs. lipid/peptide molar ratio of E2-35, E2-53R and LE-54R in three different lipid membrane models (LMM ULVs) is depicted in Figure 3 (a-c), while a comparison of the maximum % α-helicity for three peptides is shown in Figure 3 (d-f). Figures S1 and S2 display the MRE data and % structural motifs for various lipid/peptide molar ratios. Four secondary structural motifs (α-helix, β-sheet, β-turn and random coil) were fitted to the ellipticity data using Levenberg–Marquardt least squares fitting as described in Materials and Methods. Detailed information on the percentage of four secondary structural motifs present in the peptides can be found in Tables S1-S6. Our findings show that in its pure form, E2-53R exhibits a mix of β-sheet and random coil structures. On the other hand, LE-54R shows a small degree of helicity, with a higher proportion of β-sheet and random coil structures in its pure form. In contrast, when interacting with G(-) and G(+) LMMs, E2-53R and LE-54R both predominantly adopt an α-helical conformation, while in the Euk33 LMM, both adopt primarily a random coil structure. These

results highlight the influence of LMM compositions on peptide α-helicity. Interestingly, by comparing to previously published CD studies on similar linearly amphipathic peptides (LE-53 and LE-55)[94] which were not helical, addition of unnatural amino acids promotes the helical structure.

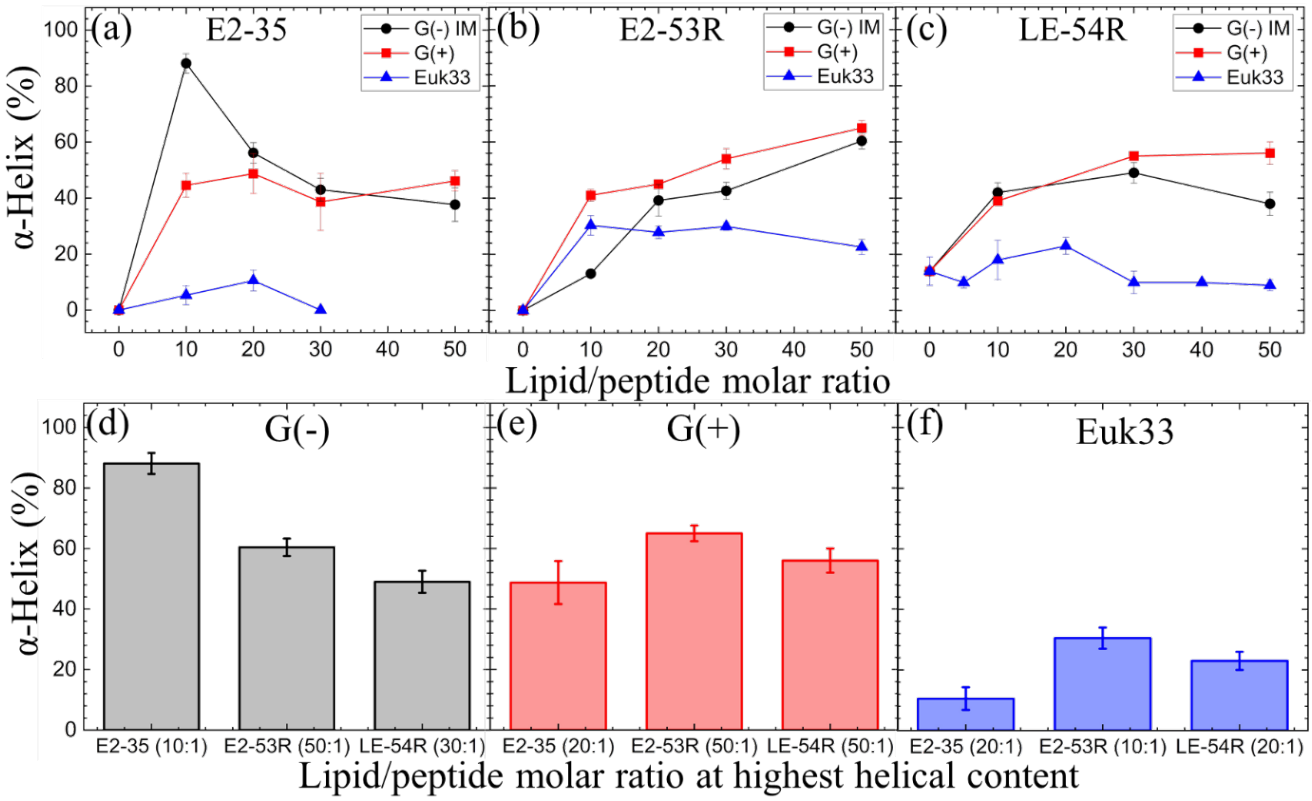

Figure 3. % α-Helix vs. lipid/peptide molar ratio of **(a)** E2-35, **(b)** E2-53R and **(c)** LE-54R in G(-) IM , G(+) and Euk33 LMMs. Summary of AMPs' helical content in three LMMs: **(d)** G(–) IM (gray), **(e)** G(+) (red), and **(f)** Euk33 (blue). The lipid/peptide molar ratio (in parentheses) is for the highest helical content. Standard deviations represent 3–4 fitting results using shape analysis. E2-35 data were adapted from our previously published paper[53] with permission.

The secondary structures of E2-53R in three LMMs are similar to the results seen with the E2-35 peptide [53], indicating that substituting tryptophan (W) and valine (V) with UAAs Tic and Nva does not greatly alter the peptide's conformation. Recently, Lu et al. studied Pep05

(KRLFKKLLKYLRKF) by substituting L-amino acid residues with D- and unnatural amino acids, such as D-lysine, D-arginine, L-2,4-diaminobutanoic acid (Dab), L-2,3-diaminopropionic acid (Dap), L-homoarginine, 4-aminobutanoic acid (Aib), and L-thienylalanine. [65] Their CD results suggested that such substitutions did not disrupt the helical structures of the peptides. [65] Likewise, Oliva et al. reported similar findings with the nona-peptide P9Nal(SS), which contained 2-naphthyl-L-alanine (Nal) and S-tert-butylthio L-cysteine. [66]

The observed helicity in E2-53R and LE-54R parallels their potent antibacterial activity. E2-53R and LE-54R both exhibit highest helicity in G(+) LMM and they are also more effective in killing G(+) bacteria as shown in Figure 2. This suggests a positive correlation of helicity with antibacterial efficacy of these peptides. The α-helical structure, where hydrophilic residues line one face and hydrophobic residues line the opposite face, facilitates peptides' interaction with membranes.[95] Certain amino acids promote helical structure, while others hinder it. [96-97] Early studies aimed at boosting membrane and antimicrobial activity involved replacing amino acids to increase helicity. [98,99-100] For instance, deleting glycine or substituting it with leucine at the N-terminus of melittin enhances its helicity and antimicrobial effectiveness. [101] Conversely, substitutions that prevent melittin from folding into a helix reduce its hemolytic and antimicrobial properties. [102-103] However, while α-helicity often corresponds to greater efficacy, there are exceptions. For instance, the D8 form of WLBU2, composed of 8 D-enantiomeric valines, exhibited a random coil structure in G(-) LMMs, unlike the predominantly helical structure of WLBU2. [34, 104] Surprisingly, both peptides showed similar efficacy in killing bacteria. Moreover, our recent findings with the linear amphipathic peptide LE-53, which possesses only β-sheet and random coil structures when interacting with bacterial membranes, demonstrated high bactericidal activity. [94] E2-53R and LE-54R both have a lower helical content in Euk33 membranes, suggesting

that cholesterol inhibits helicity. Other investigators have also studied the % helicity of AMPs vs. lipid composition with varied results.[105-106]

Peptide-Membrane Interactions

Depending on their structural characteristics, different peptides employ different mechanisms of interaction with the membrane, causing membrane alteration or permeation. [93, 107-109] Moreover, during their interactions, peptides and membranes may undergo a sequence of structural changes. Numerous studies have been carried out to clarify the interactions of peptides with lipid bilayers, which consider the position, orientation, structure, and effect on the surrounding lipids. [110-119] Therefore, a better understanding of peptide-membrane interactions at the molecular level is not only essential in the study of various biological processes, but it could also help in designing peptides with specific functionalities that may be exploited for therapeutic applications.

Membrane elasticity and lipid chain order parameter

In the present study we conducted x-ray diffuse scattering to understand the change in membrane bending modulus (K_C) and lipid chain order parameter (S_{xray}) of G(-) IM LMM with E2-53R and LE-54R. These results are compared with our previously published data of E2-35. [53] Figure 4 (a-c) show the elastic bending modulus parameter (K_C) of G(-) IM, G(+) and Euk33 LMMs with the three AMPs. A higher value of K_C indicates a stiffer membrane, and a lower value indicates a softer membrane. A general softening was observed for E2-53R and LE-54R in G(-)IM and G(+) LMMs indicating that similar softening behavior was related to their similar bactericidal activity. By contrast, K_C followed a dramatic non-monotonic behavior for E2-35 in G(-)IM and G(+) LMMs as shown in Figure 4 (a, b). We previously suggested that membrane stiffening could result from

the interaction of the AMPs with the PE component of the membranes, whereas membrane softening could result from interaction with the negatively charged lipids, PG and cardiolipin, which were tested separately.[120] This could lead to domain formation with different bending moduli in the bacterial LMMs. At the interface of these domains, defects could arise allowing leakage of ions and water through the domain wall, which would dissipate the bacterial membrane potential. However, the present study suggests that even a monotonic softening could be relevant for bacterial killing. For their interaction with Euk33 LMMs shown in Figure 4 (c), a general softening was observed for all three AMPs, but since only E2-35 is toxic to eukaryotic cells, we suggest that membrane softening is not the cause of toxicity.

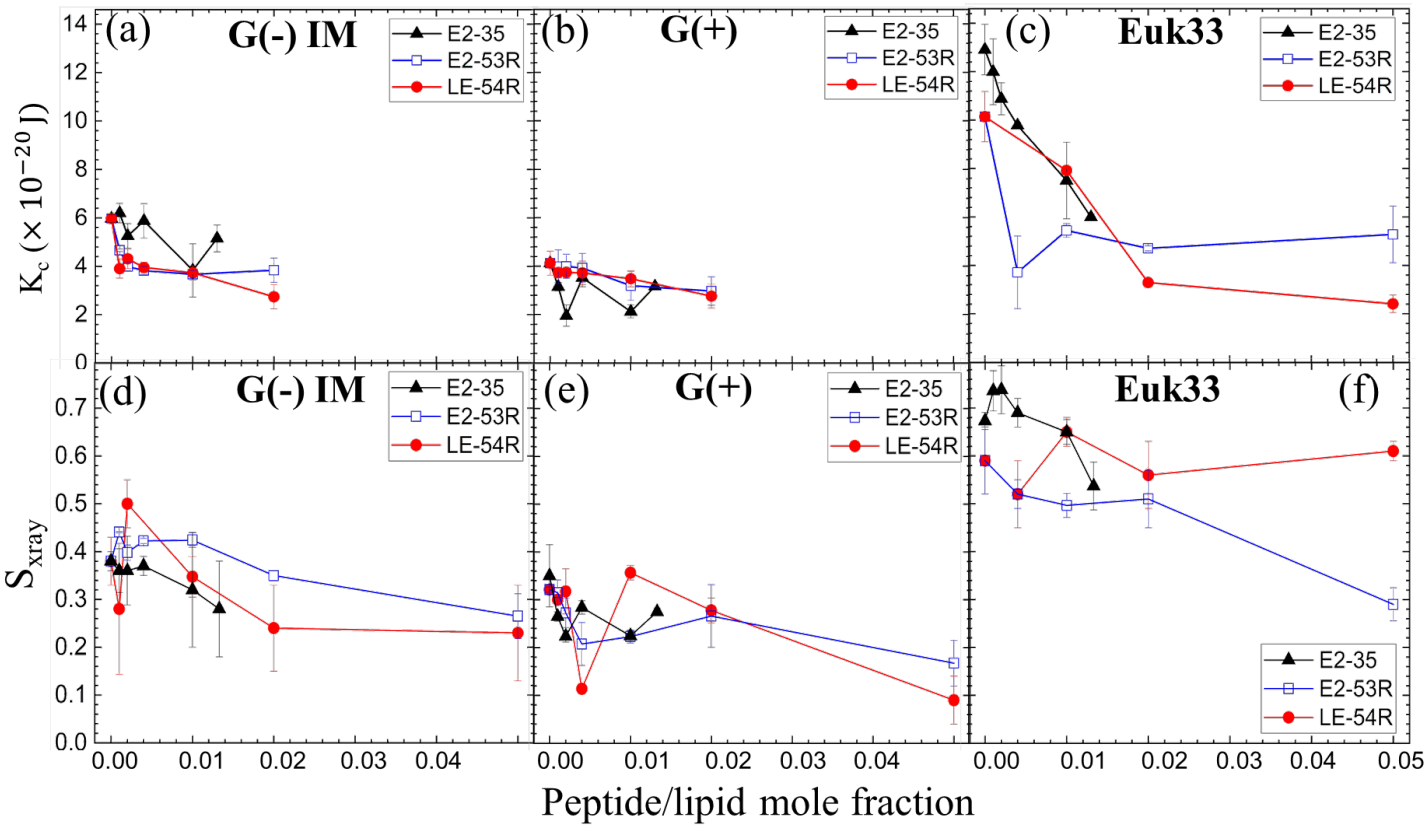

Figure 4. Bending modulus (K_C) of E2-35 (black triangles), E2-53R (hollow blue squares) and LE-54R (red circles) in **(a)** G(-) IM , **(b)** G(+) and **(c)** Euk33 LMMs. Chain order parameter (S_{xray}) of the three peptides in **(d)** G(-) IM , **(e)** G(+) and **(f)** Euk33 LMMs. (colors as in a-c). The standard deviations are from 9-18 fittings on the same sample in different positions. E2-35 data were adapted from our previously published paper [53] with permission.

In Figure 4(d to f) acyl chain order (S_{xray}) is plotted vs. peptide/lipid mole fraction. Higher values of S_{xray} signify ordered lipid acyl chains while lower values signify disordered lipid acyl chains. Both AMPs E2-53R and LE-54R caused some degree of non-monotonicity in lipid chain order similar to E2-35 indicating that lipid chain order, unlike K_C, may be related to their bacterial killing efficacies through domain formation.

Membrane structural results

With the use of the Scattering Density Profile (SDP) program we are able to locate the peptides in lipid bilayers, in order to attempt to make a correlation to bacterial killing efficacy. Figure S3 shows form factors $|F(q_z)|$, while Figure 5 presents electron density profiles (EDPs) of three LMMs for E2-35, E2-53R and LE-54R. SDP takes into account volumes of lipids, peptides, and their component groups in the bilayer, along with the number of electrons in each component. We fit the form factors by placing a Gaussian envelope for the peptide in three potential locations: the headgroup, hydrocarbon, or a combination of both, then assess the fit quality using chi-square. Generally, the SDP bilayer model fits the XDS form factor data well (Figure S3), resulting in EDPs typical of fully hydrated membranes. The various component groups in EDPs are Phos (phosphate plus outer headgroup), CG (carbonyl/glycerol), CH2 (methylene hydrocarbon region containing CH groups), CH3 (terminal methyl group), Water (fills volumes around other groups to maintain a total probability of one), and Total (sum of all component groups). Key measures derived from these EDPs include the combined peak-to-peak distance of Phos and CG (D_{HH}), and the full-width at half-maximal of the hydrocarbon region ($2D_C$), both of which indicate membrane thickness. The EDP also determines the area per lipid molecule (A_L) using lipid and peptide volumes. A summary of the XDS structural results for the three LMMs used in this study interacting with E2-53R and LE-54R is shown in Table 3.

Table 3. Summary of structural results from XDS and the charge/residue.

Sample	Area/lipid A_L [Å^2] (±1.0)	D_{HH} [Å] (± 0.5)	$2D_c$ [Å] (± 0.5)	Net charge/residue
G(-) IM control	71.0	39.2	29.1	-
G(-) IM/E2-35	75.5	38.4	27.3	-0.178
G(-) IM/E2-53R	81.0	35.3	25.5	-0.174
G(-)IM/LE-54R	74.7	36.5	27.6	-0.200
G(+) control	73.5	39.0	28.9	-
G(+)/E2-35	79.0	37.5	26.9	-0.209
G(+)/E2-53R	81.1	35.1	27.7	-0.205
G(+)/LE-54R	80.6	37.0	26.4	-0.235
Euk33 control	68.5	39.0	30.3	-
Euk33/E2-35	73.6	39.0	28.0	0.006
Euk33/E2-53R	79.9	36.6	28.0	0.010
Euk33/LE-54R	73.6	38.4	29.8	0.010

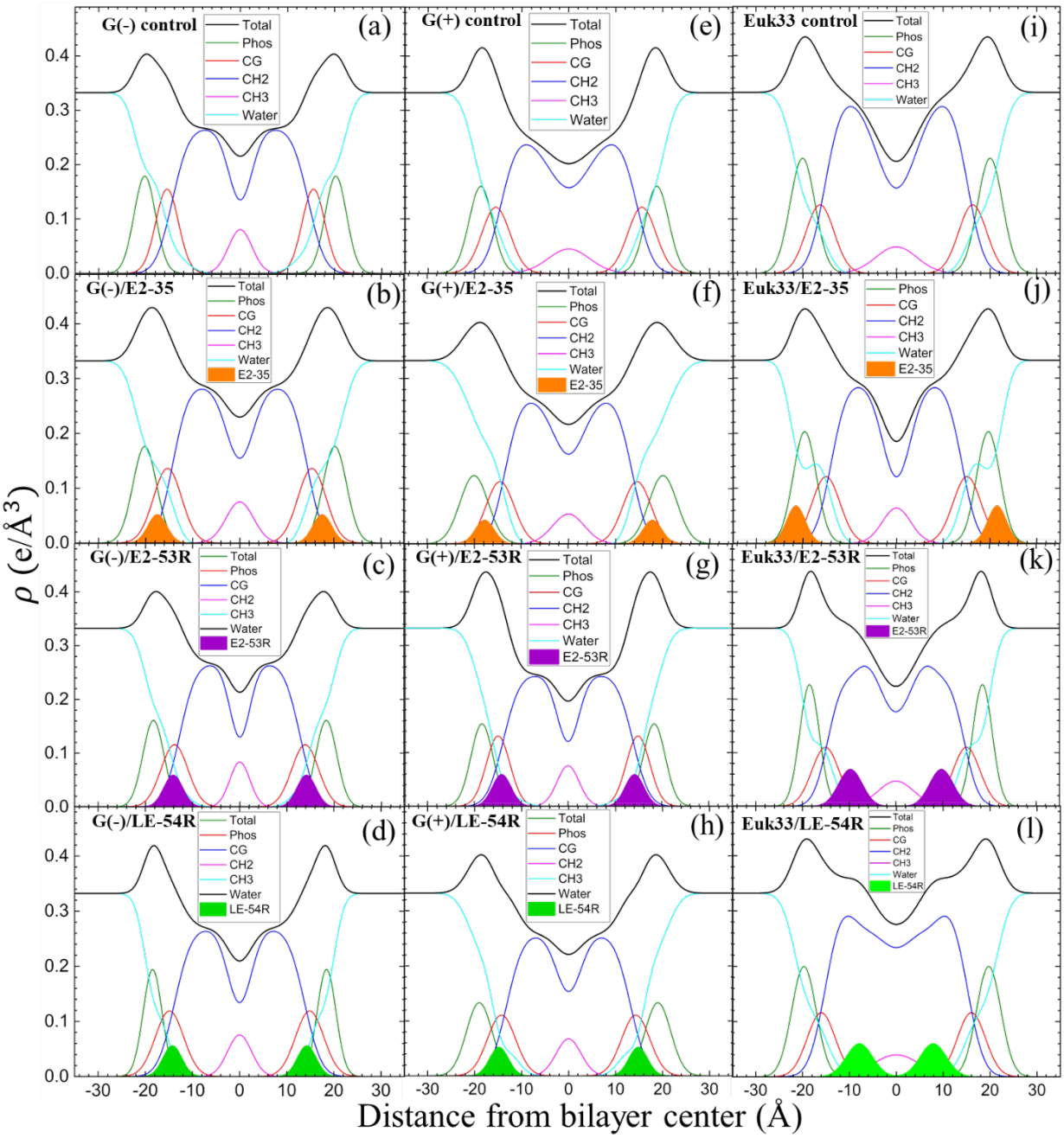

Figure 5. EDPs for G(-) IM LMMs (a to d), G(+) LMMs (e to h) and Euk33 LMMs (i to l) in the presence of E2-35, E2-53R and LE-54R. Component groups in EDPs: phosphate + external headgroup (Phos, green), carbonyl-glycerol (CG, red), CH2 (dark blue), CH3 (magenta), water (cyan), Total (black), E2-35 (filled orange), E2-53R (filled purple), LE-54R (filled lime green). Lipid/peptide molar ratio is 50:1. E2-35 data were at 75:1 and adapted from our published paper [53] with permission.

XDS data reveal that E2-53R and LE-54R locate in the interfacial region, in both G(-) and G(+) LMMs, suggesting that an interfacial location correlates with efficient bacterial killing. The reason that both peptides locate in the interfacial region could be their high arginine content, 8 arginine for E2-53R and 7 arginine for LE-54R. The amino acid arginine contains two extra nitrogens, which allow the guanidinium part of the molecule to form up to six hydrogen bonds. [121] This unique feature of arginine enables it to interact with phosphate groups in various ways, forming complexes. [122] In our recent study, we discovered that the most effective peptide, E2-35, resides under the CG Gaussian close to the interfacial region.[53] When we replaced Trp and Val of E2-35 with the unnatural amino acids Tic and Nva, there was a minor influence in the location of E2-53R in bacterial LMMs as shown in Figure 5 (c) and (g). In order to verify the locations of the peptides, we conducted NR experiments. While E2-53R and LE-54R were both studied for XDS, only E2-53R was utilized for NR, due to time constraints. NR traces are shown in Figure S4. Figure 6 provides a graphical summary of the membrane location of E2-53R in all three LMMs from NR measurements. These NR results are quantified in Table S7. As illustrated in Figure 6, the peptides' locations found by NR are in agreement with the locations determined using XDS.

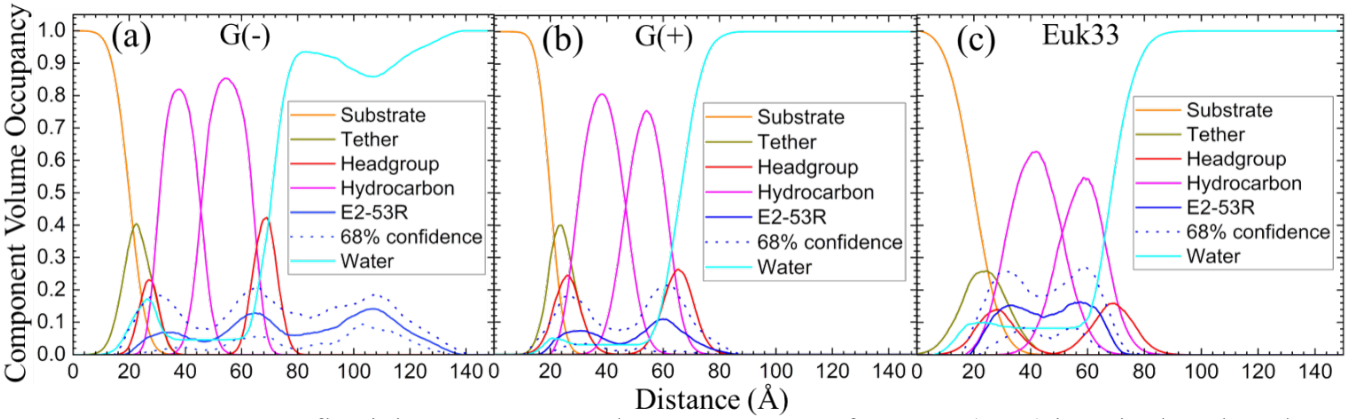

Figure 6. Neutron reflectivity component volume occupancy of E2-53R (**a – c**) in a single tethered bilayer of G(-) IM, G(+) and Euk33. Component volumes: gold-covered silicon substrate (orange), tether (olive), headgroups (red), hydrocarbons (magenta), E2-53R (blue), water (cyan). The dotted lines represent the 68 % confidence limit of the composition-space fit.

As indicated in Table 3, all three peptides decrease the thickness of the membrane (measured by $2D_C$ and D_{HH}) in both G(-) and G(+) membranes, regardless of their position within the bilayer. Likewise, the peptides increase the area per lipid (A_L) in both types of membranes. Thus, this suggests that changes in membrane thickness and area per lipid may be related to the efficient killing of bacteria exhibited by all three AMPs.

In our recent studies involving helical amphipathic (E2-35, E2-05 and E2-35K) and linear amphipathic (LE-53 and LE-55) peptides we have observed that peptides E2-35 and E2-05 which exhibit a certain level of toxicity tend to localize in the headgroup region of the Euk33 bilayer.[53] Conversely, the non-toxic peptides E2-35K, LE-53, LE-55, LE-54R and E2-53R prefer to locate within the hydrocarbon region of the lipid bilayer.[53] This suggests a correlation between the peptides' lack of toxicity and their location within the hydrocarbon region of the bilayer.

CONCLUSIONS

This study systematically examines a potential response to the escalating threat of antibiotic resistance. By investigating the efficacy of AMPs as viable alternatives, the research highlights two specific peptides with unnatural amino acids: E2-53R (16 AAs) and LE-54R (14 AAs). These UAA peptides demonstrate potent activity against both G(-) and G(+) bacteria while ensuring the safety of human cells and enhancing proteolytic resistance. Notably, both E2-53R and LE-54R maintain α-helical secondary structures when interacting with G(-) and G(+) LMMs, as revealed by CD spectroscopy. This structural feature appears to correlate with their efficacy. Additionally, XDS reveals a monotonic decrease in K_C for both peptides in G(-) and G(+) LMMs. As for lipid chain order, both E2-53R and LE-54R as well as E2-35 cause non-monotonic changes as a function of concentration, suggesting that domain formation may play a role in membrane

instability. The research also unveils a crucial link between the interfacial location of these peptides and their effectiveness, shedding light on their mode of action.

ASSOCIATED CONTENT

Data Availability Statement

The data underlying this article are available in the article and in its online Supporting Information. Any other details will be shared on reasonable request to the corresponding author.

Supporting Information

The Supporting Information is available from the ACS Library or from the corresponding author free of charge.

AUTHOR INFORMATION

Corresponding Author

Prof. Stephanie Tristram-Nagle, Biological Physics Group, Physics Department, Carnegie Mellon University, Pittsburgh, PA 15213, USA. ORCID: 0000-0003-2271-7056. Email: stn@cmu.edu

Authors

Saheli Mitra, Biological Physics Group, Physics Department, Carnegie Mellon University, Pittsburgh, PA 15213, USA. ORCID: 0000-0002-5132-3526. Email: sahelim@andrew.cmu.edu.

Mei-Tung Chen, Biological Physics Group, Physics Department, Carnegie Mellon University, Pittsburgh, PA 15213, USA. Email: meitungc@andrew.cmu.edu.

Francisca Stedman, Biological Physics Group, Physics Department, Carnegie Mellon University, Pittsburgh, PA 15213, USA. Email: fgs@andrew.cmu.edu.

Jedidiah Hernandez, Biological Physics Group, Physics Department, Carnegie Mellon University, Pittsburgh, PA 15213, USA. Email: jedidiah@andrew.cmu.edu.

Grace Kumble, Biological Physics Group, Physics Department, Carnegie Mellon University, Pittsburgh, PA 15213, USA. Email: gkumble@andrew.cmu.edu.

Xi Kang, Biological Physics Group, Physics Department, Carnegie Mellon University, Pittsburgh, PA 15213, USA. Email: xik@andrew.cmu.edu.

Churan Zhang, Biological Physics Group, Physics Department, Carnegie Mellon University, Pittsburgh, PA 15213, USA. Email: churanz@andrew.cmu.edu.

Grace Tang, Biological Physics Group, Physics Department, Carnegie Mellon University, Pittsburgh, PA 15213, USA. Email: gtang2@andrew.cmu.edu.

Ian Daugherty, Biological Physics Group, Physics Department, Carnegie Mellon University, Pittsburgh, PA 15213, USA. Email: iqd@alumni.cmu.edu.

Alice Liu, Biological Physics Group, Physics Department, Carnegie Mellon University, Pittsburgh, PA 15213, USA. Email: wanqing2@andrew.cmu.edu.

Jeremy Ocloo, Biological Physics Group, Physics Department, Carnegie Mellon University, Pittsburgh, PA 15213, USA. Email: jocloo@andrew.cmu.edu.

Kevin Raphael Klucznik, Biological Physics Group, Physics Department, Carnegie Mellon University, Pittsburgh, PA 15213, USA. Email: kkluczni@andrew.cmu.edu.

Alexander Anzhi Li, Biological Physics Group, Physics Department, Carnegie Mellon University, Pittsburgh, PA 15213, USA. Email: aal2@andrew.cmu.edu.

Frank Heinrich, Biological Physics Group, Physics Department, Carnegie Mellon University, Pittsburgh, PA 15213, USA and Center for Neutron Research, National Institute of Standards and Technology, Gaithersburg, MD 20899, USA. ORCID: 0000-0002-8579-553X. Email: fheinric@andrew.cmu.edu.

Berthony Deslouches, Department of Environmental and Occupational Health, University of Pittsburgh, Pittsburgh, PA 15261,USA. ORCID: 0000-0003-4797-7065. Email: tdesl19@pitt.edu.

Author Contributions

Investigation (SM, MC, FS, JH, GK, XK, CZ, GT, ID, FH, JO, KRK, AL, AAL, STN), data curation and formal analysis (SM, MC, FS, JH, GK, XK, CZ, GT, ID, JO, KRK, AL, AAL, FH, STN), conceptualization (SM, STN), resources (BD, STN), funding acquisition (BD, STN), supervision (SM, STN), methodology (FH, STN), Project administration (BD, STN), writing – original draft (SM, STN), writing – review & editing (MC, FS, JH, GK, XK, CZ, GT, ID, JO, KRK, AAL, FH, BD, SM, STN).

ACKNOWLEDGMENTS

This work is based upon research conducted at the Center for High Energy X-ray Sciences (CHEXS at CHESS), which is supported by the National Science Foundation under award DMR-1829070, and the Macromolecular Diffraction at CHESS (MacCHESS) facility, which is supported by award 1-P30-GM124166-01A1 from the National Institute of General Medical Sciences, National Institutes of Health, and by New York State's Empire State Development Corporation (NYSTAR). Additional support for this work was from the National Science Foundation NSF MCB-2115790 (S.M., S.T-N.), National Institute of Allergy and Infectious Diseases (NIAID) 1R01AI172861-01A1 (B.D., S.T-N.), MC and FS (SURF, CMU), JH (HURAY, CMU), GK (SURA, CMU), GT (HURAY, CMU), JO, KK, AL (SURA, CMU). F.H. was supported by the U.S. Department of Commerce (Award 70NANB17H299). The content of this publication does not necessarily reflect the views or policies of the Department of Health and Human Services, nor

does mention of trade names, commercial products, or organizations imply endorsement by the U.S. Government. The authors would like to acknowledge the ISIS facility at Rutherford Appleton Laboratory, Harwell Campus, U.K, doi:10.5286/ISIS.E.RB2310027. The authors would also like to acknowledge Dr. Stephen Paul Meisburger for his help at CHEXS (CHESS).

REFERENCES

1. Sharma, K.; Sharma, K. K.; Sharma, A.; Jain, R., Peptide-based drug discovery: Current status and recent advances. *Drug Discovery Today* **2023,** *28* (2), 103464.
2. Espeche, J. C.; Varas, R.; Maturana, P.; Cutro, A. C.; Maffía, P. C.; Hollmann, A., Membrane permeability and antimicrobial peptides: Much more than just making a hole. *Peptide Science* **2024,** *116* (1), e24305.
3. Anastasia Nijnik, L. M., Shuhua Ma,Matthew Waldbrook, Melissa R. Elliott,; Donna M. Easton, M. L. M., Sarah C. Mullaly, Jason Kindrachuk,; Håvard Jenssen, a. R. E. W. H., Synthetic Cationic Peptide IDR-1002 Provides Protection against Bacterial Infections through Chemokine Induction and Enhanced Leukocyte Recruitment. **2010,** *184*, 2539-2550.
4. Vandamme, D.; Landuyt, B.; Luyten, W.; Schoofs, L., A comprehensive summary of LL-37, the factotum human cathelicidin peptide. *Cellular immunology* **2012,** *280* (1), 22-35.
5. Erdem Büyükkiraz, M.; Kesmen, Z., Antimicrobial peptides (AMPs): A promising class of antimicrobial compounds. *Journal of Applied Microbiology* **2022,** *132* (3), 1573-1596.
6. Mba, I. E.; Nweze, E. I., Focus: Antimicrobial Resistance: Antimicrobial Peptides Therapy: An Emerging Alternative for Treating Drug-Resistant Bacteria. *The Yale journal of biology and medicine* **2022,** *95* (4), 445.
7. Hilchie, A. L.; Wuerth, K.; Hancock, R. E., Immune modulation by multifaceted cationic host defense (antimicrobial) peptides. *Nature chemical biology* **2013,** *9* (12), 761-768.
8. Wuerth, K. C.; Falsafi, R.; Hancock, R. E., Synthetic host defense peptide IDR-1002 reduces inflammation in Pseudomonas aeruginosa lung infection. *PloS one* **2017,** *12* (11), e0187565.
9. Browne, K.; Chakraborty, S.; Chen, R.; Willcox, M. D.; Black, D. S.; Walsh, W. R.; Kumar, N., A new era of antibiotics: the clinical potential of antimicrobial peptides. *International journal of molecular sciences* **2020,** *21* (19), 7047.
10. Mhlongo, J. T.; Waddad, A. Y.; Albericio, F.; de la Torre, B. G., Antimicrobial peptide synergies for fighting infectious diseases. *Advanced Science* **2023,** *10* (26), 2300472.
11. Liu, Y.; Breukink, E., The membrane steps of bacterial cell wall synthesis as antibiotic targets. *Antibiotics-Basel* **2016,** *5* (3), 28_1-22.
12. Sarkar, P.; Yarlagadda, V.; Ghosh, C.; Haldar, J., A review on cell wall synthesis inhibitors with an emphasis on glycopeptide antibiotics. *Medchemcomm* **2017,** *8* (3), 516-533.
13. Sibinelli-Sousa, S.; Hespanhol, J. T.; Bayer-Santos, E., Targeting the Achilles' heel of bacteria: different mechanisms to break down the peptidoglycan cell wall during bacterial warfare. *Journal of Bacteriology* **2021,** *203* (7), e00478-20.
14. Santos, J. A.; Lamers, M. H., Novel antibiotics targeting bacterial replicative DNA polymerases. *Antibiotics-Basel* **2020,** *9* (11), 776(1-14).
15. Kapoor, G., Saigal, S., Elongavan. A., Action and resistance mechanisms of antibiotics: A guide for clinicians. *Journal of Anaesthesiology Clinical Pharmacology* **2017,** *33*, 300-305.

16. Fernandez-Villa, D.; Aguilar, M. R.; Rojo, L., Folic acid antagonists: Antimicrobial and immunomodulating mechanisms and applications. *International Journal of Molecular Sciences* **2019,** *20* (20), 4996(1-30)
17. Deslouches, B.; Steckbeck, J. D.; Craigo, J. K.; Doi, Y.; Burns, J. L.; Montelaro, R. C., Engineered cationic antimicrobial peptides to overcome multidrug resistance by ESKAPE pathogens. *Antimicrobial agents and chemotherapy* **2015,** *59* (2), 1329-1333.
18. Stark, M.; Liu, L. P.; Deber, C. M., Cationic hydrophobic peptides with antimicrobial activity. *Antimicrobial Agents and Chemotherapy* **2002,** *46* (11), 3585-3590.
19. Stromstedt, A. A.; Ringstad, L.; Schmidtchen, A.; Malmsten, M., Interaction between amphiphilic peptides and phospholipid membranes. *Current Opinion in Colloid & Interface Science* **2010,** *15* (6), 467-478.
20. Tew, G. N.; Scott, R. W.; Klein, M. L.; DeGrado, W. F., De novo design of antimicrobial polymers, foldamers, and small molecules: from discovery to practical applications. *Accounts of chemical research* **2010,** *43* (1), 30-39.
21. Hancock, R. E., Cationic peptides: effectors in innate immunity and novel antimicrobials. *The Lancet infectious diseases* **2001,** *1* (3), 156-164.
22. Piers, K. L.; Hancock, R. E., The interaction of a recombinant cecropin/melittin hybrid peptide with the outer membrane of Pseudomonas aeruginosa. *Molecular microbiology* **1994,** *12* (6), 951-958.
23. Scott, M. G.; Yan, H.; Hancock, R. E., Biological properties of structurally related α-helical cationic antimicrobial peptides. *Infection and immunity* **1999,** *67* (4), 2005-2009.
24. Silvestro, L.; Weiser, J. N.; Axelsen, P. H., Antibacterial and antimembrane activities of cecropin A in Escherichia coli. *Antimicrobial agents and chemotherapy* **2000,** *44* (3), 602-607.
25. Matsuzaki, K.; Sugishita, K.-i.; Harada, M.; Fujii, N.; Miyajima, K., Interactions of an antimicrobial peptide, magainin 2, with outer and inner membranes of Gram-negative bacteria. *Biochimica et Biophysica Acta (BBA)-Biomembranes* **1997,** *1327* (1), 119-130.
26. Christensen, B.; Fink, J.; Merrifield, R.; Mauzerall, D., Channel-forming properties of cecropins and related model compounds incorporated into planar lipid membranes. *Proceedings of the National Academy of Sciences* **1988,** *85* (14), 5072-5076.
27. Yang, L.; Harroun, T. A.; Weiss, T. M.; Ding, L.; Huang, H. W., Barrel-stave model or toroidal model? A case study on melittin pores. *Biophysical Journal* **2001,** *81* (3), 1475-1485.
28. Velasco-Bolom, J. L.; Garduno-Juarez, R., Computational studies of membrane pore formation induced by Pin2. *Journal of Biomolecular Structure & Dynamics* **2022,** *40* (11), 5060-5068.
29. Uematsu, N.; Matsuzaki, K., Polar angle as a determinant of amphipathic alpha-helix-lipid interactions: A model peptide study. *Biophysical Journal* **2000,** *79* (4), 2075-2083.
30. Woolley, G. A.; Wallace, B. A., Model Ion Channels - Gramicidin and Alamethicin. *Journal of Membrane Biology* **1992,** *129* (2), 109-136.
31. Hallock, K. J.; Lee, D. K.; Ramamoorthy, A., MSI-78, an analogue of the magainin antimicrobial peptides, disrupts lipid bilayer structure via positive curvature strain. *Biophysical Journal* **2003,** *84* (5), 3052-3060.
32. Matsuzaki, K., Membrane permeabilization mechanisms. *Antimicrobial Peptides* **2019**, 9-16.
33. Rathinakumar, R.; Wimley, W. C., Biomolecular engineering by combinatorial design and high-throughput screening: Small, soluble peptides that permeabilize membranes. *Journal of the American Chemical Society* **2008,** *130* (30), 9849-9858.
34. Heinrich, F.; Salyapongse, A.; Kumagai, A.; Dupuy, F. G.; Shukla, K.; Penk, A.; Huster, D.; Ernst, R. K.; Pavlova, A.; Gumbart, J. C., Synergistic biophysical techniques reveal structural mechanisms of engineered cationic antimicrobial peptides in lipid model membranes. *Chemistry–A European Journal* **2020,** *26* (28), 6247-6256.

35. Chen, F. Y.; Lee, M. T.; Huang, H. W., Evidence for membrane thinning effect as the mechanism for peptide-induced pore formation. *Biophysical Journal* **2003,** *84* (6), 3751-3758.
36. Aisenbrey, C., Marquette, A., Bechinger, B., The mechanisms of action of cationic antimicrobial peptides refined by novel concepts from biophysical investigations. In *Antimicrobial Peptides Basics for Clinical Application, Advances in Experimental Medicine and Biology* KatsumiMatsuzaki, Ed. Springer Nature Singapore: Singapore, 2019; Vol. 1117, pp 33-64.
37. Epand, R. M.; Epand, R. F., Lipid domains in bacterial membranes and the action of antimicrobial agents. *Biochimica et Biophysica Acta (BBA)-Biomembranes* **2009,** *1788* (1), 289-294.
38. Shai, Y.; Oren, Z., From "carpet" mechanism to de-novo designed diastereomeric cell-selective antimicrobial peptides. *Peptides* **2001,** *22* (10), 1629-1641.
39. Yang, L.; Weiss, T. M.; Lehrer, R. I.; Huang, H. W., Crystallization of antimicrobial pores in membranes: magainin and protegrin. *Biophysical journal* **2000,** *79* (4), 2002-2009.
40. Schneider, T.; Kruse, T.; Wimmer, R.; Wiedemann, I.; Sass, V.; Pag, U.; Jansen, A.; Nielsen, A. K.; Mygind, P. H.; Raventós, D. S., Plectasin, a fungal defensin, targets the bacterial cell wall precursor Lipid II. *Science* **2010,** *328* (5982), 1168-1172.
41. Gidalevitz, D.; Ishitsuka, Y.; Muresan, A. S.; Konovalov, O.; Waring, A. J.; Lehrer, R. I.; Lee, K. Y. C., Interaction of antimicrobial peptide protegrin with biomembranes. *Proceedings of the National Academy of Sciences* **2003,** *100* (11), 6302-6307.
42. Cardon, S.; Sachon, E.; Carlier, L.; Drujon, T.; Walrant, A.; Alemán-Navarro, E.; Martínez-Osorio, V.; Guianvarc'h, D.; Sagan, S.; Fleury, Y., Peptidoglycan potentiates the membrane disrupting effect of the carboxyamidated form of DMS-DA6, a Gram-positive selective antimicrobial peptide isolated from Pachymedusa dacnicolor skin. *PLoS One* **2018,** *13* (10), e0205727.
43. Andolina, G.; Bencze, L.-C.; Zerbe, K.; Müller, M.; Steinmann, J.; Kocherla, H.; Mondal, M.; Sobek, J.; Moehle, K.; Malojcic, G., A peptidomimetic antibiotic interacts with the periplasmic domain of LptD from Pseudomonas aeruginosa. *ACS chemical biology* **2018,** *13* (3), 666-675.
44. Hancock, R. E.; Alford, M. A.; Haney, E. F., Antibiofilm activity of host defence peptides: Complexity provides opportunities. *Nature Reviews Microbiology* **2021,** *19* (12), 786-797.
45. de la Fuente-Nunez, C.; Cesaro, A.; Hancock, R. E., Antibiotic failure: Beyond antimicrobial resistance. *Drug Resistance Updates* **2023**, 101012.
46. Magana, M.; Pushpanathan, M.; Santos, A. L.; Leanse, L.; Fernandez, M.; Ioannidis, A.; Giulianotti, M. A.; Apidianakis, Y.; Bradfute, S.; Ferguson, A. L., The value of antimicrobial peptides in the age of resistance. *The lancet infectious diseases* **2020,** *20* (9), e216-e230.
47. Tan, P.; Fu, H.; Ma, X., Design, optimization, and nanotechnology of antimicrobial peptides: From exploration to applications. *Nano Today* **2021,** *39*, 101229.
48. Deslouches, B.; Phadke, S. M.; Lazarevic, V.; Cascio, M.; Islam, K.; Montelaro, R. C.; Mietzner, T. A., De novo generation of cationic antimicrobial peptides: influence of length and tryptophan substitution on antimicrobial activity. *Antimicrobial Agents and Chemotherapy* **2005,** *49* (1), 316-322.
49. Vogel, H. J.; Schibli, D. J.; Jing, W.; Lohmeier-Vogel, E. M.; Epand, R. F.; Epand, R. M., Towards a structure-function analysis of bovine lactoferricin and related tryptophan-and arginine-containing peptides. *Biochemistry and Cell Biology* **2002,** *80* (1), 49-63.
50. Xiang, W.; Clemenza, P.; Klousnitzer, J.; Chen, J.; Qin, W.; Tristram-Nagle, S.; Doi, Y.; Di, Y. P.; Deslouches, B., Rational Framework for the Design of Trp-and Arg-Rich Peptide Antibiotics Against Multidrug-Resistant Bacteria. *Frontiers in microbiology* **2022,** *13*, 889791.
51. Mandell, J. B.; Koch, J. A.; Deslouches, B.; Urish, K. L., Direct antimicrobial activity of cationic amphipathic peptide WLBU2 against Staphylococcus aureus biofilms is enhanced in physiologic buffered saline. *J Orthop Res* **2020,** *38* (12), 2657-2663.
52. Wimley, W. C.; White, S. H., Experimentally determined hydrophobicity scale for proteins at membrane interfaces. *Nature structural biology* **1996,** *3* (10), 842-848.

53. Mitra, S.; Coopershlyak, M.; Li, Y.; Chandersekhar, B.; Koenig, R.; Chen, M.-T.; Evans, B.; Heinrich, F.; Deslouches, B.; Tristram-Nagle, S., Novel Helical Trp-and Arg-Rich Antimicrobial Peptides Locate Near Membrane Surfaces and Rigidify Lipid Model Membranes. *Advanced NanoBiomed Research* **2023,** *3*, 2300013.
54. Mahlapuu, M.; Håkansson, J.; Ringstad, L.; Björn, C., Antimicrobial peptides: an emerging category of therapeutic agents. *Frontiers in cellular and infection microbiology* **2016,** *6*, 194.
55. Ong, Z. Y.; Wiradharma, N.; Yang, Y. Y., Strategies employed in the design and optimization of synthetic antimicrobial peptide amphiphiles with enhanced therapeutic potentials. *Advanced drug delivery reviews* **2014,** *78*, 28-45.
56. Biondi, B.; Casciaro, B.; Di Grazia, A.; Cappiello, F.; Luca, V.; Crisma, M.; Mangoni, M. L., Effects of Aib residues insertion on the structural–functional properties of the frog skin-derived peptide esculentin-1a (1–21) NH 2. *Amino Acids* **2017,** *49*, 139-150.
57. Khara, J. S.; Priestman, M.; Uhia, I.; Hamilton, M. S.; Krishnan, N.; Wang, Y.; Yang, Y. Y.; Langford, P. R.; Newton, S. M.; Robertson, B. D., Unnatural amino acid analogues of membrane-active helical peptides with anti-mycobacterial activity and improved stability. *Journal of Antimicrobial Chemotherapy* **2016,** *71* (8), 2181-2191.
58. Sun, S.; Zhao, G.; Huang, Y.; Cai, M.; Yan, Q.; Wang, H.; Chen, Y., Enantiomeric effect of d-Amino acid substitution on the mechanism of action of α-helical membrane-active peptides. *International journal of molecular sciences* **2017,** *19* (1), 67.
59. Zaet, A.; Dartevelle, P.; Daouad, F.; Ehlinger, C.; Quilès, F.; Francius, G.; Boehler, C.; Bergthold, C.; Frisch, B.; Prévost, G., D-Cateslytin, a new antimicrobial peptide with therapeutic potential. *Scientific reports* **2017,** *7* (1), 15199.
60. Zhong, C.; Zhu, N.; Zhu, Y.; Liu, T.; Gou, S.; Xie, J.; Yao, J.; Ni, J., Antimicrobial peptides conjugated with fatty acids on the side chain of D-amino acid promises antimicrobial potency against multidrug-resistant bacteria. *European Journal of Pharmaceutical Sciences* **2020,** *141*, 105123.
61. Wang, X.; Yang, X.; Wang, Q.; Meng, D., Unnatural amino acids: Promising implications for the development of new antimicrobial peptides. *Critical Reviews in Microbiology* **2023,** *49* (2), 231-255.
62. Sarkar, T.; Chetia, M.; Chatterjee, S., Antimicrobial peptides and proteins: From nature's reservoir to the laboratory and beyond. *Frontiers in Chemistry* **2021,** *9*, 691532.
63. Agostini, F.; Völler, J. S.; Koksch, B.; Acevedo-Rocha, C. G.; Kubyshkin, V.; Budisa, N., Biocatalysis with unnatural amino acids: enzymology meets xenobiology. *Angewandte Chemie International Edition* **2017,** *56* (33), 9680-9703.
64. Barrett, G., *Chemistry and biochemistry of the amino acids*. Springer Science & Business Media: 2012; p 684.
65. Lu, J.; Xu, H.; Xia, J.; Ma, J.; Xu, J.; Li, Y.; Feng, J., D-and unnatural amino acid substituted antimicrobial peptides with improved proteolytic resistance and their proteolytic degradation characteristics. *Frontiers in Microbiology* **2020,** *11*, 563030.
66. Oliva, R.; Chino, M.; Pane, K.; Pistorio, V.; De Santis, A.; Pizzo, E.; D'Errico, G.; Pavone, V.; Lombardi, A.; Del Vecchio, P., Exploring the role of unnatural amino acids in antimicrobial peptides. *Scientific Reports* **2018,** *8* (1), 8888.
67. Wang, C.; Hong, T.; Cui, P.; Wang, J.; Xia, J., Antimicrobial peptides towards clinical application: Delivery and formulation. *Advanced drug delivery reviews* **2021,** *175*, 113818.
68. Russell, A. L.; Kennedy, A. M.; Spuches, A. M.; Gibson, W. S.; Venugopal, D.; Klapper, D.; Srouji, A. H.; Bhonsle, J. B.; Hicks, R. P., Determining the effect of the incorporation of unnatural amino acids into antimicrobial peptides on the interactions with zwitterionic and anionic membrane model systems. *Chemistry and physics of lipids* **2011,** *164* (8), 740-758.

69. Hicks, R. P.; Abercrombie, J.; Wong, R.; Leung, K., Antimicrobial peptides containing unnatural amino acid exhibit potent bactericidal activity against ESKAPE pathogens. *Bioorganic & medicinal chemistry* **2013,** *21* (1), 205-214.
70. Travkova, O. G.; Moehwald, H.; Brezesinski, G., The interaction of antimicrobial peptides with membranes. *Advances in colloid and interface science* **2017,** *247*, 521-532.
71. D'souza, A. R.; Necelis, M. R.; Kulesha, A.; Caputo, G. A.; Makhlynets, O. V., Beneficial impacts of incorporating the non-natural amino acid azulenyl-alanine into the Trp-rich antimicrobial peptide buCATHL4B. *Biomolecules* **2021,** *11* (3), 421.
72. Wilkinson, S. G., *Microbial Lipids*. Academic Press: San Diego, CA, 1988; Vol. 1.
73. Gottfried, E. L., Lipids of human leukocytes: relation to cell type. *Journal of lipid research* **1967,** *8* (4), 321-327.
74. Branzoi, I.; Iordoc, M.; Branzoi, F.; Vasilescu-Mirea, R.; Sbarcea, G., Influence of diamond-like carbon coating on the corrosion resistance of the NITINOL shape memory alloy. *Surface and Interface Analysis* **2010,** *42* (6-7), 502-509.
75. Deslouches, B.; Steckbeck, J. D.; Craigo, J. K.; Doi, Y.; Mietzner, T. A.; Montelaro, R. C., Rational design of engineered cationic antimicrobial peptides consisting exclusively of arginine and tryptophan, and their activity against multidrug-resistant pathogens. *Antimicrobial agents and chemotherapy* **2013,** *57* (6), 2511-2521.
76. Deslouches, B.; Hasek, M. L.; Craigo, J. K.; Steckbeck, J. D.; Montelaro, R. C., Comparative functional properties of engineered cationic antimicrobial peptides consisting exclusively of tryptophan and either lysine or arginine. *Journal of medical microbiology* **2016,** *65* (6), 554.
77. Brahms, S.; Brahms, J., Determination of protein secondary structure in solution by vacuum ultraviolet circular dichroism. *Journal of molecular biology* **1980,** *138* (2), 149-178.
78. Tristram-Nagle, S. A., Preparation of oriented, fully hydrated lipid samples for structure determination using X-ray scattering. *Methods Mol Biol* **2007,** *400*, 63-75.
79. Kučerka, N.; Tristram-Nagle, S.; Nagle, J. F., Closer look at structure of fully hydrated fluid phase DPPC bilayers. *Biophysical journal* **2006,** *90* (11), L83-L85.
80. Lyatskaya, Y.; Liu, Y.; Tristram-Nagle, S.; Katsaras, J.; Nagle, J. F., Method for obtaining structure and interactions from oriented lipid bilayers. *Physical Review E* **2000,** *63* (1), 011907.
81. De Gennes, P.-G.; Prost, J., *The physics of liquid crystals*. Oxford university press: 1993.
82. Mills, T. T.; Toombes, G. E.; Tristram-Nagle, S.; Smilgies, D.-M.; Feigenson, G. W.; Nagle, J. F., Order parameters and areas in fluid-phase oriented lipid membranes using wide angle X-ray scattering. *Biophysical journal* **2008,** *95* (2), 669-681.
83. Inc, M., MATLAB, Version: 9.13. 0 (R2022b). **2022**.
84. Dalgliesh, R.; Langridge, S.; Plomp, J.; De Haan, V.; Van Well, A., Offspec, the ISIS spin-echo reflectometer. *Physica B: Condensed Matter* **2011,** *406* (12), 2346-2349.
85. Budvytyte, R.; Valincius, G.; Niaura, G.; Voiciuk, V.; Mickevicius, M.; Chapman, H.; Goh, H.-Z.; Shekhar, P.; Heinrich, F.; Shenoy, S., Structure and properties of tethered bilayer lipid membranes with unsaturated anchor molecules. *Langmuir* **2013,** *29* (27), 8645-8656.
86. Eells, R.; Hoogerheide, D. P.; Kienzle, P. A.; Lösche, M.; Majkrzak, C. F.; Heinrich, F., Structural investigations of membrane-associated proteins by neutron reflectometry. *Characterization of Biological Membranes: Structure and Dynamics; Nieh, M.-P., Heberle, FA, Katsaras, J., Eds* **2019**, 87-130.
87. Shekhar, P.; Nanda, H.; Lösche, M.; Heinrich, F., Continuous distribution model for the investigation of complex molecular architectures near interfaces with scattering techniques. *Journal of applied physics* **2011,** *110* (10).
88. Heinrich, F.; Lösche, M., Zooming in on disordered systems: Neutron reflection studies of proteins associated with fluid membranes. *Biochimica et Biophysica Acta (BBA)-Biomembranes* **2014,** *1838* (9), 2341-2349.

89. Fauchere, J. L.; Pliska, V., Hydrophobic parameters-Pi of amino-acid side-chains from the partitioning of N-acetyl-amino-acid amides. *Eur J Med Chem* **1983,** *18* (4), 369-375.
90. Eisenberg, D.; Weiss, R. M.; Terwilliger, T. C., The helical hydrophobic moment - a measure of the amphiphilicity of a helix. *Nature* **1982,** *299* (5881), 371-374.
91. Gautier, R.; Douguet, D.; Antonny, B.; Drin, G., HELIQUEST: a web server to screen sequences with specific α-helical properties. *Bioinformatics* **2008,** *24* (18), 2101-2102.
92. Matsuzaki, K., Why and how are peptide–lipid interactions utilized for self-defense? Magainins and tachyplesins as archetypes. *Biochimica et Biophysica Acta (BBA)-Biomembranes* **1999,** *1462* (1-2), 1-10.
93. Zasloff, M., Antimicrobial peptides of multicellular organisms. *nature* **2002,** *415* (6870), 389-395.
94. Mitra, S.; Chandersekhar, B.; Li, Y.; Coopershlyak, M.; Mahoney, M. E.; Evans, B.; Koenig, R.; Hall, S.; Klösgen, B. M.; Heinrich, F., Novel non-helical antimicrobial peptides insert into and fuse lipid model membranes. *Soft Matter* **2024**.
95. Kabelka, I.; Vacha, R., Advances in Molecular Understanding of α-Helical Membrane-Active Peptides. *Accounts of Chemical Research* **2021,** *54* (9), 2196-2204.
96. Dathe, M.; Wieprecht, T., Structural features of helical antimicrobial peptides: their potential to modulate activity on model membranes and biological cells. *Biochimica et Biophysica Acta (BBA)-Biomembranes* **1999,** *1462* (1-2), 71-87.
97. Mai, X. T.; Huang, J. F.; Tan, J. J.; Huang, Y. B.; Chen, Y. X., Effects and mechanisms of the secondary structure on the antimicrobial activity and specificity of antimicrobial peptides. *Journal of Peptide Science* **2015,** *21* (7), 561-568.
98. Ciulla, M. G.; Gelain, F., Structure–activity relationships of antibacterial peptides. *Microbial Biotechnology* **2023,** *16* (4), 757-777.
99. Mangoni, M. L.; Carotenuto, A.; Auriemma, L.; Saviello, M. R.; Campiglia, P.; Gomez-Monterrey, I.; Malfi, S.; Marcellini, L.; Barra, D.; Novellino, E., Structure− activity relationship, conformational and biological studies of temporin L analogues. *Journal of medicinal chemistry* **2011,** *54* (5), 1298-1307.
100. Chen, H.-C.; Brown, J. H.; Morell, J. L.; Huang, C., Synthetic magainin analogues with improved antimicrobial activity. *Febs Letters* **1988,** *236* (2), 462-466.
101. Mojsoska, B.; Jenssen, H., Peptides and peptidomimetics for antimicrobial drug design. *Pharmaceuticals* **2015,** *8* (3), 366-415.
102. Xu, X.; Lai, R., The chemistry and biological activities of peptides from amphibian skin secretions. *Chemical reviews* **2015,** *115* (4), 1760-1846.
103. Chen, N.; Jiang, C., Antimicrobial peptides: Structure, mechanism, and modification. *European Journal of Medicinal Chemistry* **2023,** *255*, 115377.
104. Di, Y.; Lin, Q.; Chen, C.; Montelaro, R.; Doi, Y.; Deslouches, B., Enhanced therapeutic index of an antimicrobial peptide in mice by increasing safety and activity against multidrug-resistant bacteria. *Science advances* **2020,** *6* (18), eaay6817.
105. Sani, M. A.; Whitwell, T. C.; Separovic, F., Lipid composition regulates the conformation and insertion of the antimicrobial peptide maculatin 1.1. *Biochimica Et Biophysica Acta-Biomembranes* **2012,** *1818* (2), 205-211.
106. Fleming, E.; Maharaj, N. P.; Chen, J. L.; Nelson, R. B.; Elmore, D. E., Effect of lipid composition on buforin II structure and membrane entry. *Proteins-Structure Function and Bioinformatics* **2008,** *73* (2), 480-491.
107. Shai, Y., Mechanism of the binding, insertion and destabilization of phospholipid bilayer membranes by α-helical antimicrobial and cell non-selective membrane-lytic peptides. *Biochimica et Biophysica Acta (BBA)-Biomembranes* **1999,** *1462* (1-2), 55-70.
108. Ergene, C.; Yasuhara, K.; Palermo, E. F., Biomimetic antimicrobial polymers: Recent advances in molecular design. *Polymer Chemistry* **2018,** *9* (18), 2407-2427.

109. Li, W.; Separovic, F.; O'Brien-Simpson, N. M.; Wade, J. D., Chemically modified and conjugated antimicrobial peptides against superbugs. *Chemical Society Reviews* **2021,** *50* (8), 4932-4973.
110. Ciumac, D.; Gong, H.; Hu, X.; Lu, J. R., Membrane targeting cationic antimicrobial peptides. *Journal of colloid and interface science* **2019,** *537*, 163-185.
111. Gera, S.; Kankuri, E.; Kogermann, K., Antimicrobial peptides–unleashing their therapeutic potential using nanotechnology. *Pharmacology & Therapeutics* **2022,** *232*, 107990.
112. Cardoso, P.; Glossop, H.; Meikle, T. G.; Aburto-Medina, A.; Conn, C. E.; Sarojini, V.; Valery, C., Molecular engineering of antimicrobial peptides: Microbial targets, peptide motifs and translation opportunities. *Biophysical reviews* **2021,** *13*, 35-69.
113. Hall, B. A.; Chetwynd, A. P.; Sansom, M. S., Exploring peptide-membrane interactions with coarse-grained MD simulations. *Biophysical journal* **2011,** *100* (8), 1940-1948.
114. Sato, H.; Feix, J. B., Peptide–membrane interactions and mechanisms of membrane destruction by amphipathic α-helical antimicrobial peptides. *Biochimica et Biophysica Acta (BBA)-Biomembranes* **2006,** *1758* (9), 1245-1256.
115. Gan, B. H.; Gaynord, J.; Rowe, S. M.; Deingruber, T.; Spring, D. R., The multifaceted nature of antimicrobial peptides: Current synthetic chemistry approaches and future directions. *Chemical Society Reviews* **2021,** *50* (13), 7820-7880.
116. Booth, V.; Warschawski, D. E.; Santisteban, N. P.; Laadhari, M.; Marcotte, I., Recent progress on the application of H-2 solid-state NMR to probe the interaction of antimicrobial peptides with intact bacteria. *Biochimica Et Biophysica Acta-Proteins and Proteomics* **2017,** *1865* (11), 1500-1511.
117. Marquette, A.; Bechinger, B., Biophysical investigations elucidating the mechanisms of action of antimicrobial peptides and their synergism. *Biomolecules* **2018,** *8* (2), 18(1-22).
118. Leber, R.; Pachler, M.; Kabelka, I.; Svoboda, I.; Enkoller, D.; Vacha, R.; Lohner, K.; Pabst, G., Synergism of antimicrobial frog peptides couples to membrane intrinsic curvature strain. *Biophysical Journal* **2018,** *114* (8), 1945-1954.
119. Buck, A. K.; Elmore, D. E.; Darling, L. E. O., Using fluorescence microscopy to shed light on the mechanisms of antimicrobial peptides. *Future Medicinal Chemistry* **2019,** *11* (18), 2447-2460.
120. Dupuy, F. G.; Pagano, I.; Andenoro, K.; Peralta, M. F.; Elhady, Y.; Heinrich, F.; Tristram-Nagle, S., Selective interaction of colistin with lipid model membranes. *Biophysical journal* **2018,** *114* (4), 919-928.
121. Hristova, K.; Wimley, W. C., A look at arginine in membranes. *The Journal of membrane biology* **2011,** *239* (1), 49-56.
122. Allolio, C.; Magarkar, A.; Jurkiewicz, P.; Baxova, K.; Javanainen, M.; Mason, P. E.; Sachl, R.; Cebecauer, M.; Hof, M.; Horinek, D.; Heinz, V.; Rachel, R.; Ziegler, C. M.; Schrofel, A.; Jungwirth, P., Arginine-rich cell-penetrating peptides induce membrane multilamellarity and subsequently enter via formation of a fusion pore. *P Natl Acad Sci USA* **2018,** *115* (47), 11923-11928.